Int J Adv Manuf Technol (2017) 91:3933–3941
DOI 10.1007/s00170-017-0062-2

ORIGINAL ARTICLE

Experimental study on cutting performance of microwave sintered Ti(C, N)/Al2O3 cermet tool in the dry machining of hardened steel

Yong Zhang[1,2] · **Yu Cheng**[1,2] · **Hanpeng Hu**[1,2] · **Zengbin Yin**[1,2]

Received: 5 August 2016 / Accepted: 16 January 2017 / Published online: 2 February 2017

Abstract A kind of Ti(C, N)/Al_2O_3 composite cermet tool was prepared by microwave sintering. The cutting performance and wear mechanisms were investigated via high speed dry cutting of hardened steel 40Cr (AISI 5140) in comparison with those of two kinds of conventional cemented carbide tools YS8 and YT15. The optimal cutting parameters were obtained by orthogonal array and range analysis, in which the optimum objectives were material removal, surface roughness, and tool life. The results indicated that the optimal cutting parameters of the cermet tool were the cutting speed of 120 m/min, the depth of cut of 0.3 mm, and the feed rate of 0.1 mm/rev. Compared to the cemented carbide tools, the tool life of the cermet tool is 64.5 min, which is about 115.0% higher than YS8 and 168.8% than YT15. The average surface roughness is 1.27 μm, which is about 15.9% lower than that of the cemented carbide tools. The cermet tool shows much better cutting performance than those of cemented carbide tools. The failure mode of the microwave sintered Ti(C,N)/Al_2O_3 cermet tool was micro-chipping, and the wear mechanisms were mainly abrasion wear and adhesive abrasion.

Keywords Ti(C,N)/Al_2O_3 cermet tool · Microwave sintering · Dry cutting · Cutting performance · Wear mechanisms

✉ Yu Cheng
chengyu106@mail.njust.edu.cn

[1] Nanjing University of Science & Technology, School of Mechanical Engineering, Nanjing 210094, People's Republic of China

[2] Collaborative Innovation Center of High-End Equipment Manufacturing Technology, Ministry of Industry and Information Technology, Nanjing University of Science and Technology, Nanjing 210094, People's Republic of China

1 Introduction

In recent years, turning of hardened steels with high efficiency and quality is a topic of great interest in industrial production and scientific research. Hardened steels are widely used in the automotive, gear, bearing, tool, and die industry for their high hardness and wear resistance [1, 2]. Generally, hardened steels are processed by grinding, but grinding has the shortcomings of low efficiency, environment pollution, and the long processing cycle [3]. With the development of cutting technology, high-speed dry cutting gradually becomes one of the process techniques in finishing due to the advantages of high efficiency and nonpollution [4, 5]. However, high-speed dry cutting leads to high cutting temperature, which accelerate the tool wear. So, the performances of tool material are vital to the application of this production method.

Various cutting tools have been used in dry cutting of hardened steel. Polycrystalline cubic boron nitride (PCBN) [6–8] and ceramic tools [9, 10] are commonly used in today's industrial production. PCBN tools have high hardness and excellent thermal conductivity, but the high cost of PCBN tools has shifted the challenge for dry cutting from economic viability. The mechanical properties of ceramic tools are similar to PCBN, but the wide application of ceramic tools has been limited due to their low toughness. Ti(C, N)-based cermet, which is made of ceramic phase (Ti(C,N) or a mixture of TiC and TiN) and metal binder phase (Ni or a mixture of Co and Ni), possesses several attractive properties, such as high-temperature hardness, excellent wear resistance, plastic deformation resistance, chemical stability, and low friction coefficient against metals [11–14]. It is considered to be a potential tool for dry cutting of hardened steels [15–17].

Table 1 Characteristics and composition ratios of the starting powders for cermet tool materials

Power	Grain size(μm)	Purity (wt.%)	Manufacturer	Composition ratios (wt.%)
Ti(C, N)(C:*N* = 7:3)	0.2	99.9	Shanghai	44
WC	2	99.9	Shanghai	10
Mo_2C	2.5	99	Shanghai	10
Co	2	99.5	Shanghai	7.5
Ni	2	99.5	Shanghai	7.5
α-Al_2O_3	0.6	99.9	Shanghai	21

However, as the workpiece becomes harder and tougher, the cutting temperature at chip-tool interfacing can reach above 1000 °C during dry machining, and high temperature mechanical properties of tools are becoming more important. Consequently, it is necessary to improve the hardness and abrasion of Ti(C, N)-based cermet tools. Some researches have suggested that incorporating Al_2O_3 particles into Ti(C, N)-based cermet can obviously enhance the hardness and high-temperature mechanical properties, leading to the improvement of the wear resistance. Xu et al. [18] studied the effects of Al_2O_3 particles on the mechanical properties of Ti(C, N)-based cermet tool materials which were densified using hot-pressed sintering. The optimal mechanical properties were gained with 12 wt.% Al_2O_3; the bending strength, hardness, and fracture toughness were 900 MPa, 17.4 GPa, and 9.95 MPa·$m^{1/2}$; and the Al_2O_3 particles can cause the grain fining effect and improve the mechanical properties. Meng et al. [19] investigated the high-temperature tribological behaviors of two hot pressing TiCN-based cermets, namely TiCN-Ni-Mo and TiCN-Al_2O_3-Ni-Mo; the results showed that TiCN-Al_2O_3-Ni-Mo with 10 wt.% Al_2O_3 exhibited higher hardness and wear resistance than TiCN-Ni-Mo.

It is well known that hot pressed sintering technology is the main method of preparing Ti(C, N)-based cermet [16, 20, 21]. However, the heat is generated by heating element, and then transferred to the specimen from the surfaces to the inside though heat conduction and thermal stress can be induced due to the temperature gradient during the heat transfer process, which influence the mechanical properties of ceramic material. In comparison with traditional sintering technology, microwave sintering is a process in which heat is produced as a result of coupling reaction between the whole specimen and electromagnetic wave [22–24]. Therefore, heating is more rapid with energy saved, and a homogeneous temperature distribution within the materials is achievable. Additionally, microwave electromagnetic can decrease sintering activation energy of the material, increase the grain-boundary diffusion, and accelerate the sintering process; so, the crystalline structure can be refined and properties have been efficiently improved [25, 26].

In our previous research, Ti(C, N)-based cermet tool materials have been successfully fabricated by microwave sintering, and their mechanical properties were discussed, but the hardness is only 15.49 GPa, which is not effective for high-speed cutting hardened steel [27]. In this study, the Ti(C, N)/Al_2O_3 cermet tool strengthened by Al_2O_3 particles was firstly fabricated by microwave sintering. The cutting performance and wear mechanisms of the microwave sintered Ti(C, N)/Al_2O_3 cermet tool were investigated via high-speed dry cutting of hardened steel, with the conventional cemented carbide tools YS8 and YT15 used as competitors.

2 Experimental procedures

2.1 Preparation of Ti(C, N)/Al_2O_3 cermet tools

Characteristics and composition ratios of the starting powders for Ti(C, N)/Al_2O_3 cermet tool materials are listed in Table 1. The mixed powders were ball milled with alumina grinding media in planetary ball mill (Model QM-3SP2, Nanjing, China) for 24 h, and then, 3 wt.% PVA with a concentration of 5 wt.% was added to the mixed powders as binder for 2 h. Subsequently, the mixed powders were dried in a vacuum

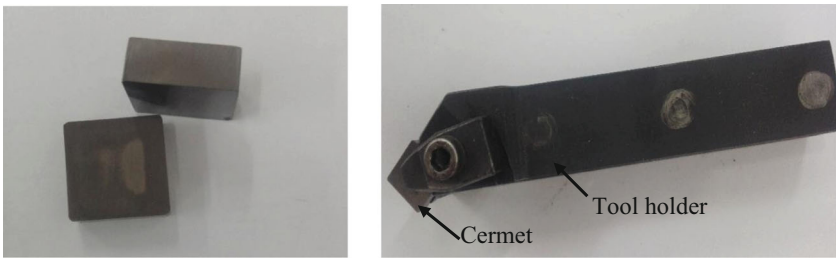

Fig. 1 The cermet tool and the insert with tool holder

Table 2 Physical and mechanical properties of the tools

Tools	Density (g/cm^3)	Vickers hardness (GPa)	Facture toughness (MPa/m$^{1/2}$)
Cermet	5.704	17.78 ± 0.2	8.65 ± 0.55
YS8	12.87	15.3 ± 0.7	13.12 ± 0.21
YT15	11.6	14.9 ± 0.4	11.71 ± 0.32

Table 3 Tool geometries of the cermet, YS8, and YT15

Tools	Rake angle γ_0	Flank angle α_0	Cutting edge angle κ_r	Inclination angle λ_0	Tool nose radius (mm) γ_ε (mm)
Cermet	−5°	5°	45°	−5°	0.1
YS8	−5°	10°	45°	−2°	1
YT15	−5°	10°	45°	−2°	1

drying oven (Model DZF-1, Shanghai, China), and then sieved through a 100 mesh for further use.

The dried powders were placed in a cold steel die, and then pressed uniaxially at 280~320 MPa for 2 min. Then, the compacts were sintered in a 2.45-GHz microwave furnace (Model NJZ-1, Nanjing, China) at 1550 °C with the holding time of 10 min under N_2 atmosphere. The microwave generators were operated with power output in the range 0–6 KW, and the average heating rate was about 50–80 °C/min. After that, the compacts were milled on a tool grinder until they met the needs of cutters. The cermet tool and the insert with tool holder are shown in Fig. 1.

2.2 Cutting experiments

In this paper, cutting performance of the cermet tool was tested in comparison with commercial cemented carbide tools YS8 (94%WC–6%Co) and YT15 (15%TiC–79%WC–6%Co) which was provided by Zhuzhou Cemented Carbide Works. Cemented carbide tools with ISO designation of 513-2004 and YS8 meet the ISO M05 and YT15 meets the ISO P10. Physical and mechanical properties of the three tool materials are listed in Table 2, and the geometries are compiled to Table 3. As the compressive stress strength of the cermet tool is higher than that of bending strength, using negative rake angle is preferred, for negative angle can translate the tensile stress to pressure stress and breakage of the tool could be avoided during cutting.

A hardened steel 40Cr (AISI 5140) with a diameter of 110 mm and a length of 400 mm was chosen as the workpiece at the present experimentation. This material was selected on account of its application in crank shafts, transmission shaft, gear and worm requiring high hardness and wear resistance. It was hardened and tempered to 50 ± 2 HRC. The chemical compositions (wt.%) of the workpiece are given in Table 4.

Orthogonal array was taken to evaluate the cutting performance. The optimum objectives were material removal (V), surface roughness (Ra), and tool life (T). The cutting parameters and parameter levels are listed in Table 5. The optimum cutting parameters of the cermet tool were determined by range analysis. The wear mechanisms of the tools were analyzed, and the tool life was compared.

The cutting experiments were performed under dry condition on a CK6140 lathe. The flank wear (VB) of cutting tool was measured by Dino-Lite stereomicroscope (AM3113T, Tai wan). The average surface roughness (Ra) of machined workpiece was measured by roughmeter (Taylor, Surtronic 25, UK). The wear micrographs of the worn out tools were examined using scanning electron microscopy (SEM, Quant 250FEG, USA). Dispersive X-ray spectroscopy (EDS) analysis has been carried out to make the chemical analysis of the cutting tool. Flank wear was measured at intervals, and the value of 0.3 mm was used as tool life criterion.

3 Results and discussion

3.1 Cutting performance in turning steel

The experimental results for continuous dry turning of hardened steel 40Cr (AISI 5140) with the cermet tool are illustrated in Table 6. With the metal removal as the optimum objective, maximum metal removal can be obtained under the cutting condition of v = 120 m/min, f = 0.125 mm/rev,

Table 4 Chemical compositions (wt.%) of workpiece material

Chemical element	C	Si	Mn	Cr	S	P	Fe
Content (wt.%)	0.38~0.43	0.15~0.35	0.7~0.9	0.7~0.9	≤0.040	≤0.035	Bal.

Table 5 Cutting parameters and their levels

Parameters	Symbol	Unit	Levels		
			1	2	3
Cutting speed	v	m/min	120	180	240
Feed rate	f	mm/r	0.1	0.125	0.15
Depth of cut	a_p	mm	0.1	0.2	0.3

a_p = 0.3 mm. The relation of range analysis for cutting parameters is R(a_p) > R(f) ≈ R(v), and the depth of cut has a significant effect on metal removal. However, when cutting at v = 120 m/min, f = 0.125 mm/rev, a_p = 0.3 mm, the average surface roughness is 2.443 μm, which cannot meet the requirement of finishing. For the surface roughness, the relation of range analysis is R(f) > R(v) > R(a_p) from Table 6, and the feed rate is the main factor, which has significant effect on the surface roughness. Figure 2 shows the effect of single factor for cutting parameters on surface roughness and tool life. It is observed that the tool life had a sharp decrease with an increase of cutting speed as shown in Fig. 2a. The tool life decreased from 81.77 to 39.47 min, while cutting speed increased from 120 to 240 m/min. This is mainly attributed to the high cutting force and cutting heat caused by high cutting speed. It is noticed that the surface roughness increased rapidly with the increase of feed rate from Fig. 2c. The high scallop machine may be the reason for the phenomenon. In Fig. 2b, surface roughness maintained similar with the increase of the depth of cut. Therefore, big depth of cut, low cutting speed, and feed rate should be chosen to ensure machining quality and high turning efficiency. As a result, the optimal cutting parameters are selected as v = 120 m/min, a_p = 0.3 mm, and f = 0.1 mm/rev.

Experimental results of the three tools after dry turning of hardened steel 40Cr (AISI 5140) under the optimal cutting parameters are listed in Table 7. Compared to cemented carbide tools YS8 and YT15, the cutting time of the cermet tool is 64.5 min, which is about 115.0% higher than YS8 and 168.8% than YT15. Moreover, the metal removal is 1,326,383 mm^3,

Table 6 Results for orthogonal experiment and range analysis

Test.no		v(m/min)	a_p(mm)	f(mm/r)	Metal removal	Surface roughness	Cutting time
		A	B	C	V (mm^3)	R_a (μm)	T (min)
1		120	0.1	0.1	503,311	1.027	101.5
2		120	0.2	0.125	904,320	1.548	76.9
3		120	0.3	0.15	1,215,270	2.443	66.9
4		180	0.1	0.125	635,741	1.841	75.5
5		180	0.2	0.15	835,569	2.545	44
6		180	0.3	0.1	968,708	1.103	49.9
7		240	0.1	0.15	580,257	3.568	43.2
8		240	0.2	0.1	836,647	1.118	50
9		240	0.3	0.125	857,838	1.744	25.2
V	K_1	2,622,901	1,719,309	2,308,666	∑ = 7,337,661		
	K_2	2,440,018	2,576,536	2,397,899			
	K_3	2,274,742	3,041,816	2,631,096			
	$\overline{K}_1$	874,300	573,103	769,555			
	$\overline{K}_2$	813,339	858,845	799,300			
	$\overline{K}_3$	758,247	1,013,939	877,032			
R		116,053	440,839	107,477			
Ra	K_1	5.018	6.436	3.248	∑ = 16.937		
	K_2	5.489	5.211	5.133			
	K_3	6.43	5.29	8.556			
	$\overline{K}_1$	1.673	2.145	1.083			
	$\overline{K}_2$	1.83	1.737	1.711			
	$\overline{K}_3$	2.413	1.763	2.852			
R		0.74	0.408	1.749			

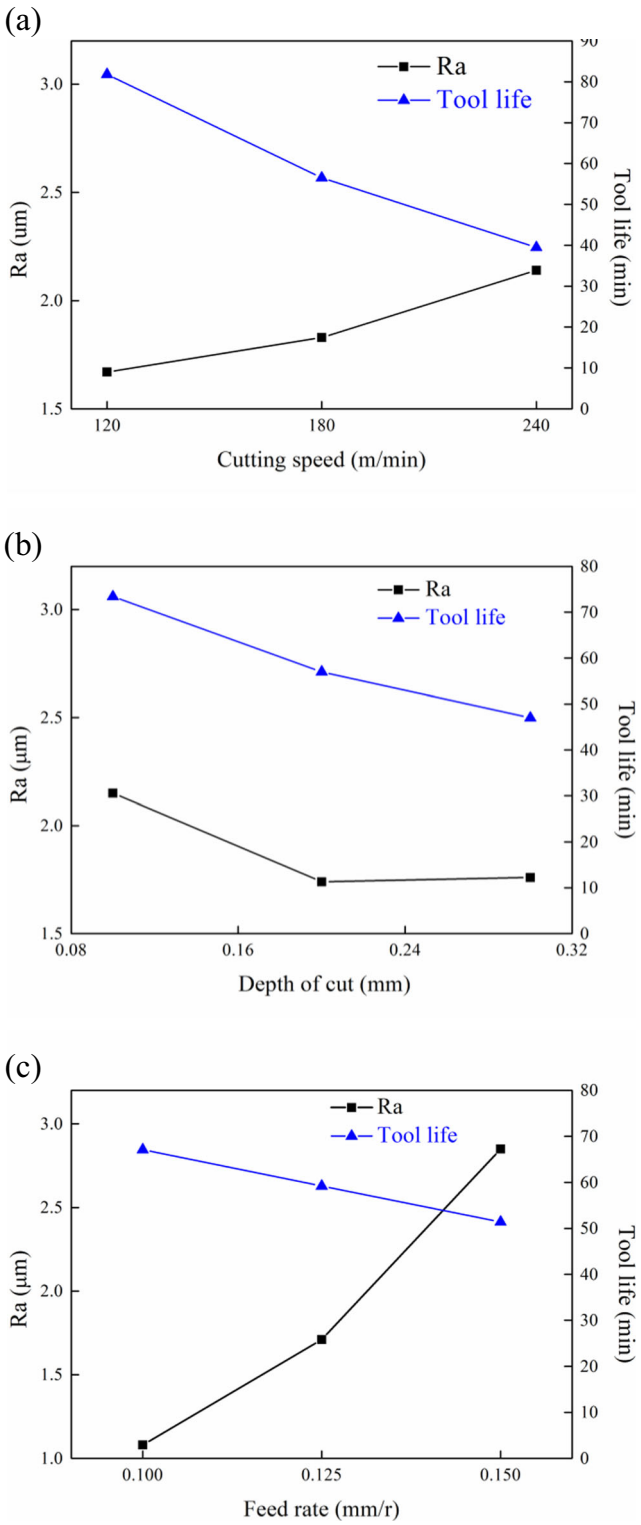

Fig. 2 Effect of **a** cutting speed, **b** depth of cut, **c** feed rate on surface roughness and tool life

and average surface roughness is 1.27 μm, which is about 15.9% lower than cemented carbide tools YS8 and YT15. The cermet tool showed much better cutting performance than

Table 7 Experimental results of the tools under the optimal cutting parameters

Tools	V (mm^3)	Ra (μm)	T (min)
Cermet	1,326,383	1.27	64.5
YS8	416,612	1.51	30.0
YT15	316,102	1.51	24.0

cemented carbide tools. On one hand, the high temperature of such cermet tools has been improved due to the incorporation of Al_2O_3 particle, which is higher than that of the cemented carbide tools. Although the fracture toughness is lower than that of YS8 and YT15, it is still acceptable. Al_2O_3 particles are useful to enhance the wear resistance of the Ti(C, N)/Al_2O_3 composite cermet tool. On the other hand, the surface frictional forces for the cermet tool are lower than those of cemented carbide tools. WC which is the main composition of cemented carbide tools has good affinity with Fe. Moreover, Ti(C, N)

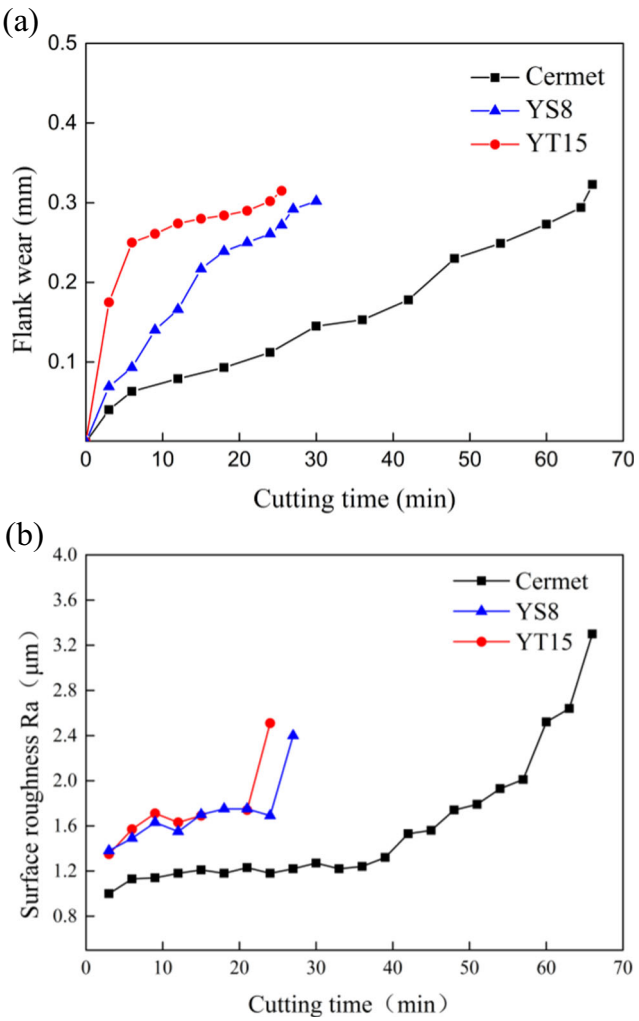

Fig. 3 Curves of **a** flank wear (VB) and **b** surface roughness (Ra) vary with the cutting time

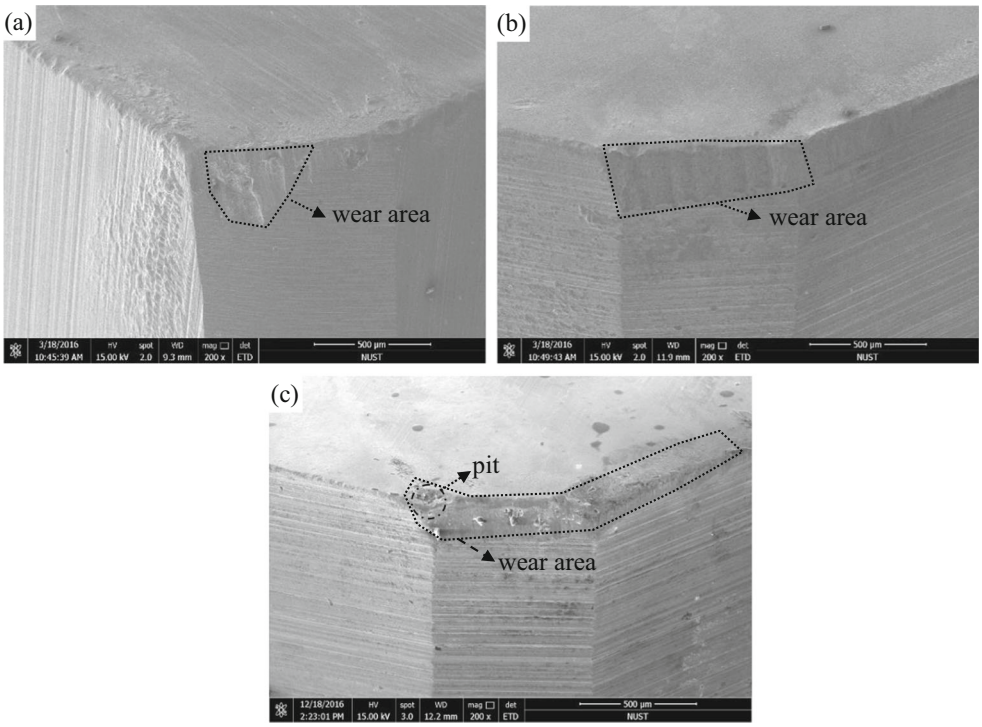

Fig. 4 SEM micrographs of tool nose for **a** cermet, **b** YS8, **c** YT15

has high thermal conductivity, and TiO_2 can be formed over the cutting surface and prevent the matrix material from adhesive abrasion in some degree [15]; so, the finish quality of the steel is high.

The curves of flank wear (VB) and surface roughness (Ra) that vary with the cutting time are grouped in Fig. 3. It is observed that the cermet tool shows much longer endurance than YS8 and YT15 from Fig. 3a, and the endurance of YS8 and YT15 is similar under this cutting condition. Apparently, the curve of the cermet tool is relatively smooth, and the flank wear is only 0.294 mm until 64.5 min. Some studies have shown that abrasion resistance of tool material not only has effect on the grain size but also has relationship with the mechanical properties of tool material [19]. The incorporation of Al_2O_3 has improved the mechanical properties and wear resistance of the cermet tool. The Fig. 3b shows that surface roughness of the cermet tool is lower than YS8 and YT15, for the hard phase in cemented carbide has high friction coefficient with the workpiece, and that is not conducive to the surface quality. It is worth noting that the surface roughness of the cermet tool changed slightly before 57 min but increased rapidly in the later period. That may be attributed to the micro-chipping on the flank of tool.

3.2 Wear mechanisms

The SEM micrographs of tool nose for the three tools after dry turning of hardened steel 40Cr (AISI 5140) are shown in Fig. 4. The wear area of cemented carbide tools YS8 (Fig. 4b) and YT15 (Fig. 4c) is larger than that of the cermet tool (Fig. 4a). However, surface spalling can be seen from Fig. 4a. In contrast, a large-scale pit occurred on the tool nose of YT15 as shown in Fig. 4c (marked by black circle). The high stress concentration of tool nose may be the reason for the phenomenon.

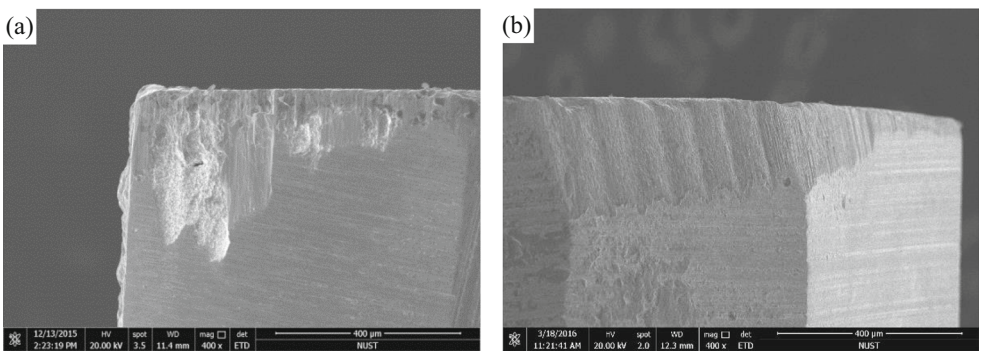

Fig. 5 SEM images of flank wear for **a** cermet and **b** YS8

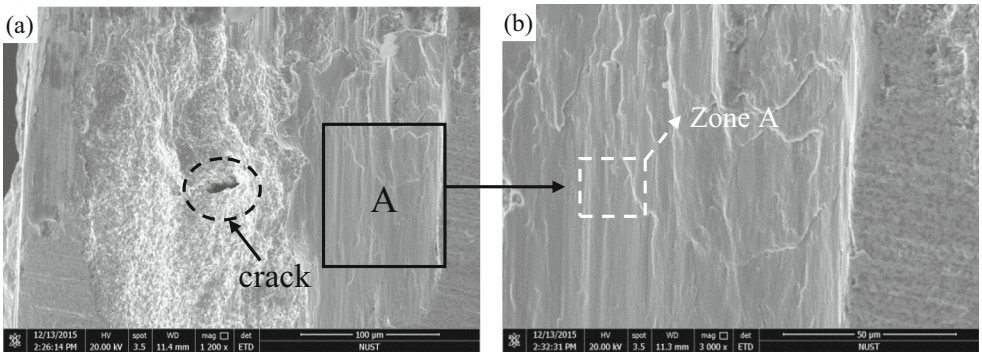

Fig. 6 SEM micrographs of worn area for **a** cermet and **b** magnification of area A

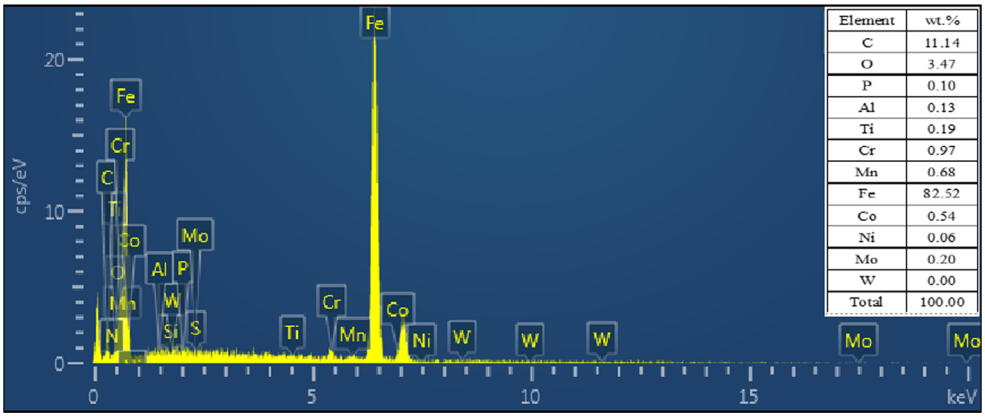

Fig. 7 EDS analysis of zone A

The SEM images of flank wear for the cermet tool and YS8 after dry turning of hardened steel 40Cr (AISI 5140) at the optimal cutting parameters are shown in Fig. 5a, b. It is clearly seen that micro-chipping occurred on the flank face of the cermet tool from Fig. 5a, and chipping took place in the wear land near the tool nose. This is due to the micro-plastic deformation of the tool face repeatedly effected by polytropic contact pressure and shear stress during turning; the cutting heat on the tool nose could hardly be eliminated, and thermal stress concentration will generate on the tool face. Finally, thermal stress together with cutting force induces the interior crack growth and the micro-chipping happened. The micro-chipping is also responsible for the sudden decline of surface roughness after 50 min as shown in Fig. 3b. The failure mode of the YS8 is wear, the wear band is rather long, and plowing groove has generated on the flank face (Fig. 5b) for its low thermostability, poor hardness, and wear resistance.

Figure 6 shows the SEM micrographs of flank face for the cermet tool. Crack in the material is observed (black mark in Fig. 6a), and the crack under the sustained action of applied load would degrade the bond strength between the particles, which can also accelerate tool failure. Figure 5b shows the magnified part of area A on Fig. 6a. It can be seen that there are some adhesive coating that took place on the worn area. EDS analysis of the adhesive coating (zone A) is shown in Fig. 7. As the element of Fe content reached up to 85.52%, it can be concluded that the adhesive coating is from smear metal, which can be considered as an indication of adhesive

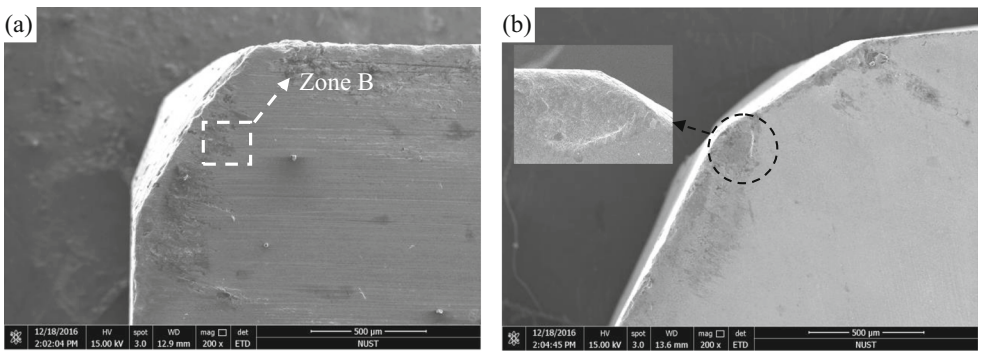

Fig. 8 SEM micrographs of rake face for **a** cermet and **b** YT15. The *black circle* indicates crater wear

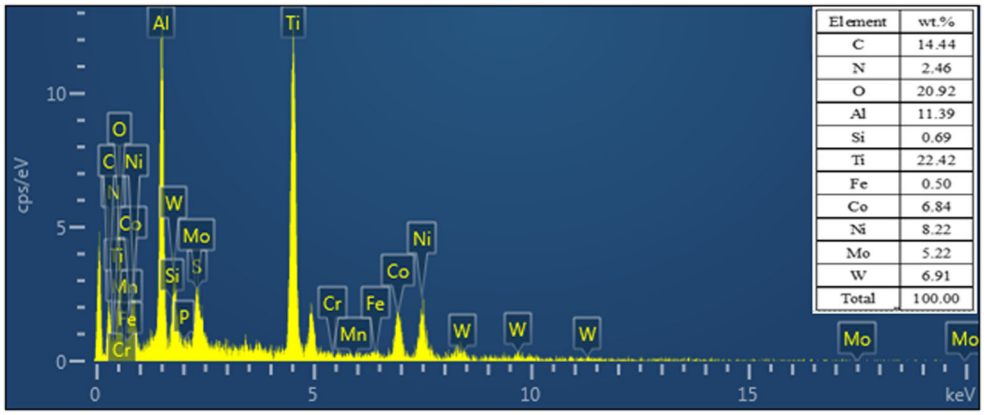

Fig. 9 EDS analysis of zone B

wear. Moreover, scratch can be clearly seen on the built up layers, which suggests that the abrasive wear occurred during the turning. The reason for the scratch should be the abrasion of the soft phase from the tool and hard particles from the workpiece and flowing chips during the turning.

The SEM micrographs of rake face for the cermet tool and YT15 are shown in Fig. 8. There is no distinct scratch on the rake face of the cermet tool from Fig. 8a, whereas evident crater wear is on the rake face of YT15 as shown in Fig. 8b. Based on the EDS analysis of zone B (Fig. 9), the content of Fe was 0.5% merely and the vast majority is matrix element. The fact suggested that no adhesive wear occurred on the rack face of the cermet tool.

4 Conclusions

The cutting performance and wear mechanisms of microwave sintered Ti(C,N)/Al_2O_3 cermet tool were investigated via the dry turning of hardened steel 40Cr (AISI 5140). Several conclusions were drawn based on the experimental results:

(1) Microwave sintered Ti(C, N)/Al_2O_3 cermet tool is appropriate for dry turning of hardened steel 40Cr (AISI 5140). When setting the metal removal, surface roughness of workpiece, and tool life as the optimization objective, the optimal cutting parameters are v = 120 m/min, a_p = 0.3 mm, and f = 0.1 mm/rev.

(2) At the optimal cutting parameters, tool life of the cermet tool was 64.5 min, which is about 115.0% higher than YS8 and 168.8% than YT15, the cermet tool shows much higher endurance and well machinability than YS8 and YT15. Moreover, average surface roughness of the workpiece for the cermet tool is 1.27 μm; turning instead of grinding can be achieved.

(3) The cermet tool shows higher wear resistance than YS8 and YT15. The failure mode of the cermet tool is microchipping in turning hardened steel 40Cr (AISI 5140), and the wear mechanisms are abrasion wear and adhesive abrasion.

Acknowledgements The work is supported by the National Natural Science Foundation of China (51505227), Natural Science Foundation of Jiangsu Province of China (BK20150783), and the Fundamental Research Funds for the Central Universities (30915118809).

References

1. Zhou JM, Andersson M, Ståhl JE (2004) Identification of cutting errors in precision hard turning process. J Mater Process Technol 153(2–3):746–750
2. Elbestawi MA, Chen L, Becze CE, El-Wardany T (1997) High-speed milling of dies and molds in their hardened state. CIRP Ann Manuf Technol 46(1):57–62
3. Poulachon G, Bandyopadhyay BP, Jawahir IS, Pheulpin S, Seguin E (2004) Wear behavior of CBN tools while turning various hardened steels. Wear 256(3–4):302–310
4. Sreejith PS, Ngoi BKA (2000) Dry machining: machining of the future. J Mater Process Technol 101(1–3):287–291
5. Kumar BVM, Kumar JR, Basu B (2007) Crater wear mechanisms of TiCN–Ni–WC cermets during dry machining. Int J Refrac Met 25(5):392–399
6. Coelho RT, Ng EG, Elbestawi MA (2007) Tool wear when turning hardened AISI 4340 with coated PCBN tools using finishing cutting conditions. Int J Mach Tools Manuf 47(2):263–272
7. Sobiyi K, Sigalas I, Akdogan G, Turan Y (2015) Performance of mixed ceramics and CBN tools during hard turning of martensitic stainless steel. Int J Adv Manuf Technol 77(5):861–871
8. Oliveira AJD, Boing D, Schroeter RB (2016) Effect of PCBN tool grade and cutting type on hard turning of high-chromium white cast iron. Int J Adv Manuf Technol 82(5):797–807
9. Aslantas K, Ucun I, Çicek A (2012) Tool life and wear mechanism of coated and uncoated Al_2O_3/TiCN mixed ceramic tools in turning hardened alloy steel. Wear 274-275(3):442–451
10. Barry J, Byrne G (2001) Cutting tool wear in the machining of hardened steels: part I: alumina/TiC cutting tool wear. Wear 247(2):139–151
11. Ahn SY, Kim SW, Kang S (2001) Microstructure of Ti(CN)–WC–NbC–Ni cermets. J Am Ceram Soc 84(4):843–849
12. Zhou H, Huang C, Zou B, Liu HL, Zhu HT, Yao P, Wang J (2014) Effects of metal phases and carbides on the microstructure and mechanical properties of Ti(C,N)-based cermets cutting tool materials. Mater Sci Eng A 618:462–470

13. Alvarez M, Sánchez JM (2007) Spark plasma sintering of Ti(C, N) cermets with intermetallic binder phases. Int J Refrac Met 25(1): 107–118
14. Canteli JA, Cantero JL, Marín NC, Gómez B, Gordo E, Miguéle MH (2010) Cutting performance of TiCN–HSS cermet in dry machining. J Mater Process Technol 210(1):122–128
15. Liu N, Chao S, Yang HD (2006) Cutting performances, mechanical property and microstructure of ultra-fine grade Ti(C, N)-based cermets. Int J Refrac Met Hard Mater 24(6):445–452
16. Zou B, Zhou H, Xu KT, Huang CZ, Wang J, Li SS (2014) Study of a hot-pressed sintering preparation of Ti(C7N3)-based composite cermets materials and their performance as cutting tools. J Alloys Compd 611:363–371
17. Aslantas K, Ucun I (2009) The performance of ceramic and cermet cutting tools for the machining of austempered ductile iron. Int J Adv Manuf Technol 41(7):642–650
18. Xu LQ, Wang SL, Huang CZ, Hou ZG, Liu HL (2008) Influence of Nano-scale Al_2O_3 on the properties of Ti(C,N)-based cermet. Rare Metal Mat Eng 37(4):732–735
19. Meng J, Lu J, Wang J, Yang S (2006) Tribological behavior of TiCN-based cermets at elevated temperatures. Mater Sci Eng A 418(1–2):68–76
20. Russias J, Cardinal S, Esnouf C, Fantozzi G, Bienvenu K (2007) Hot pressed titanium nitride obtained from SHS starting powders: influence of a pre-sintering heat-treatment of the starting powders on the densification process. J Eur Ceram Soc 27(1):327–335
21. Monteverde F, Medri V, Bellosi A (2002) Microstructure of hot-pressed Ti(C,N)-based cermets. J Eur Ceram Soc 22(14):2587–2593
22. Roy R, Agrawal D, Amp JC, Gedevanishvili S (1999) Full sintering of powdered-metal bodies in a microwave field. Nature 399(6750): 304–304
23. Acevedo L, Usón S, Uche J (2014) Exergy transfer analysis of microwave heating systems. Energy 68(68):349–363
24. Zuo F, Bade A, Saunier S, Goeuriot D, Heuguet R (2014) Microwave versus conventional sintering: estimate of the apparent activation energy for densification of α-alumina and zinc oxide. J Eur Ceram Soc 34(12):3103–3110
25. Demirskyi D, Agrawal D, Ragulya A (2014) Tough ceramics by microwave sintering of nanocrystalline titanium diboride ceramics. Ceram Int 40(1):1303–1310
26. Janney MA, Kimrey HD, Schmidt MA, Kiggans JO (1991) Grain growth in microwave-annealed alumina. J Am Ceram Soc 74(7): 1675–1681
27. Hu HP, Cheng Y, Yin ZB, Zhang Y, Lu TY (2015) Mechanical properties and microstructure of Ti(C, N) based cermet cutting tool materials fabricated by microwave sintering. Ceram Int 41(10): 15017–15023